A Reduced Order Model for Nonlinear Dynamics of Mistuned Bladed Disks With Shroud Friction Contacts

S. Mehrdad Pourkiaee, Stefano Zucca

A reduced order model for nonlinear dynamics of mistuned bladed disks with shroud friction contacts

S. Mehrdad Pourkiaee[1*], Stefano Zucca[1]

[1]Department of Mechanical and Aerospace Engineering, Politecnico di Torino, Corso Duca degli Abruzzi 24, Torino 10129, Italy

Abstract

A new reduced order modeling technique for nonlinear vibration analysis of mistuned bladed disks with shrouds is presented. The developed reduction technique employs two component mode synthesis methods, namely, the Craig-Bampton (CB) method followed by a modal synthesis based on loaded interface modeshapes (Benfield and Hruda). In the new formulation the fundamental sector is divided into blade and disk components. The CB method is applied to the blade, where nodes lying on shroud contact surfaces and blade-disk interfaces are retained as master nodes, while modal reductions is performed on the disk sector with loaded interfaces. The use of loaded interface component modes allows removing the blade-disk interface nodes from the set of master nodes retained in the reduced model. The result is a much more reduced order model with no need to apply any secondary reduction. In the paper it is shown that the reduced order model of the mistuned bladed disk can be obtained with only single-sector calculation, so that the full finite element model of the entire bladed disk is not necessary. Furthermore, with the described approach it is possible to introduce the blade frequency mistuning directly into the reduced model. The nonlinear forced response is computed using the harmonic balance method (HBM) and alternating frequency/time domain (AFT) approach. Numerical simulations revealed the accuracy, efficiency and reliability of the new developed technique for nonlinear vibration analysis of mistuned bladed disks with shroud friction contacts.

[*] Address all correspondence to this author.

Emails:
mehrdad.pourkiaee@polito.it
stefano.zucca@polito.it

1 Introduction

Bladed disks are critical turbomachinery components, subjected to oscillating forces arisen from different sources (e.g. unbalancing, fluctuating fluid pressures), which can cause their failure due to high cycle fatigue [1]. Bladed disk design requires forced response analysis to be performed in the frequency range where resonance conditions are expected, according to preliminary modal analysis [2]. Due to the presence of contact interfaces (such as shrouds, blade-disk joints, bolted flanges, friction dampers) the dynamic behavior of bladed disks is nonlinear and in order to correctly assess the damping level provided by the interfaces, which limits the vibration amplitude and the related stresses, nonlinear calculations are necessary [3]. In the last three decades, nonlinear methods [4] based on harmonic balance method (HBM) have established themselves as highly accurate and numerically efficient methods to compute the steady-state response of assemblies with contact interfaces, such as bladed disks [5]. Despite the huge time savings achievable by using the HBM with respect to Time Domain Analysis (TDA), the typical size of industrial finite element (FE) models of bladed disks (i.e. millions of degrees of freedom per sector) makes the analysis unfeasible for design purposes, unless reduced order models (ROMs) are implemented to shorten the computational time.

The above describes scenario, which applies to any structure with contact interfaces, becomes even more challenging for bladed disks, because of the unavoidable mistuning, which characterizes them. In the literature, with the word mistuning [6] researchers mean the small differences, which exist between the blades due to geometrical tolerances, material inhomogeneity, assembly process, wear phenomena, etc.

The random nature of mistuning and its extreme effects on the bladed disk response require statistical analysis of the dynamic behavior of the bladed disks [7]. In the literature, a large number of papers are available describing efficient ROMs for the linear forced response of mistuned bladed disks in case

of small mistuning [8]-[13]. The basic idea; the available ROMs are based on; is that the modeshapes of the tuned system (i.e. bladed disk with identical blades) can be used as a basis for reduction of the corresponding full mistuned system. In other words, the mistuned vibration modes can be projected to the normal modes of the corresponding tuned system. This hypothesis implies that one can compute the reduction basis (i.e. the modeshapes of the tuned system) only once at the beginning of the forced response analysis, by performing single sector (called fundamental sector) computations, with the appropriate cyclic symmetry boundary conditions, without any need to develop the FE model of the full system.

One cannot naturally extend the ROMs developed for linear systems to the nonlinear case, since:

1. There is no proof that any set of modeshapes of the tuned system are a suitable basis for nonlinear forced response.
2. The equivalent stiffness provided by the contact interfaces depends on the vibration amplitude and therefore there is not a single tuned linear system suitable as a projection basis for the governing equations of the nonlinear mistuned system.

The literature about nonlinear mistuned bladed disks is much smaller, compared to the literature on linear mistuned systems [6] and nonlinear tuned systems [5], the reasons for that being the difficulties either in performing nonlinear analyses of full systems or in developing effective ROMs for the mistuned system. In [14] the nonlinear forced response of mistuned bladed disks was investigated for the first time, by updating the FRF matrix of the linear system with the Woodbury-Sherman-Morrison formula [11], while in [15] the approach was applied to investigate high-mode vibrations. In [16] an updated FRF matrix formulation is used with the Woodbury-Sherman-Morrison formula to generate a reduced set of governing equations of the nonlinear forced response of bladed disks. In both cases, at each frequency, the FRF matrix used in the governing equations of the system is updated in order to introduce mistuning in the bladed disk model at specific locations by means of mistuning elements. In reference [17] it is shown that sets of modeshapes (Adaptive Microslip Projections) computed from

multiple linear systems can be efficiently used as a reduction basis for mistuned bladed disks with contact interfaces in order to investigate the system dynamics [18].

In this paper, a ROM for the nonlinear analysis of mistuned bladed disks is presented. In its development, the following requirements are taken into account:

1. The ROM must be obtained by performing only single-sector calculations.
2. Mistuning is modelled as blade frequency mistuning (i.e. by perturbing the blades Young's modulus).
3. It is preferable that the whole reduction is performed once, and then blade frequency mistuning is introduced directly in the ROM.
4. If requirement 3 is not fulfilled, then any numerical operation (i.e. those performed per each mistuning pattern) must be cheap enough to justify the adoption of the ROM.
5. The ROM must allow for physical degrees of freedom (DOFs) to be retained only at the contact interfaces for the purpose of nonlinear forced response analysis.

A Component Mode Synthesis (CMS) approach is used and the bladed disk is divided into its components: the disk and a set of N blades. It is well known in the literature that any time a CMS approach is used, the interface degrees of freedom (DOFs) of the components may become the largest portion of the ROM, although their contribution to the dynamics of the system may be marginal. In order to overcome this problem, interface reduction methods have been developed [19]-[23] to reduce the size of the interface DOFs.

In this paper a novel approach is applied to the mistuned bladed disks with friction contacts with the objective of eliminating the blade-disk interfaces from the final ROM. The developed approach results in further reduced ROMs with no need of secondary reduction techniques. The adopted logic implies that in the presence of friction contacts such as shrouds and underplatform dampers, the friction damping at the blade root joints is negligible and one can model the blade-disk joint as perfectly linearly elastic.

In detail, the blades are reduced with the Craig-Bampton (CB-CMS) approach [24], retaining as master DOFs, shroud contact DOFs and interface DOFs between blades and the disk. Then, after performing the so-called primal assembly between the reduced blades and the full disk; at the interface DOFs; the loaded interface modeshapes of the disk are used to approximate the dynamics of the disk and interfaces. Here, loaded interface modeshapes refer to normal modes of the disk component where blades are statically condensed (loaded) on blade-disk interfaces [25]. The resulting ROM only retains as master DOFs the contact DOFs and, if deemed necessary by the analyst, additional auxiliary DOFs on the blades.

Finally, it is shown that, the CB-CMS reduction matrix of the blades is invariant with respect to the blade frequency mistuning. Accordingly, in the case of small mistuning, a general formulation is derived which enables analysts and designers to obtain the mistuned ROM of the full system based on sector level calculations.

In the paper, the method is described by using as a reference a mock-up bladed disk with shrouded blades. Contact interfaces are modeled by imposing a 3D contact element (comprised of two perpendicular Jenkins contact elements with variable normal loads), at each retained contact node. Nonlinear forced response is computed using the HBM method and the alternating frequency/time domain (AFT) approach [26]. Numerical simulations revealed the accuracy and the reliability of the new developed technique in predicting the nonlinear response levels of mistuned shrouded bladed disks with friction interfaces.

2 Reduced order modeling technique

In order to better clarify the mathematical formulation of the reduced order model, the method is firstly applied to a single sector (i.e. disk fundamental sector + 1 blade) and only afterwards it is shown how to extend the sector reduced matrices to the full system and how to introduce blade mistuning into the final reduced system.

2.1 Methodology

In the newly developed reduction technique, the fundamental sector of a tuned bladed disk is divided into blade and disk components. First, the CB-CMS reduction is applied to the blade component. Then the modal reduction is performed to project the physical interface and disk DOFs onto the modal coordinates of the disk loaded interface modeshapes. As a preliminary step, the blade and the disk sector DOFs and their corresponding stiffness matrices are partitioned as follows:

$$x_B = \begin{Bmatrix} x_I \\ x_N \\ x_\gamma^b \end{Bmatrix}, K_b = \begin{bmatrix} k_{II}^b & k_{IN}^b & k_{I\gamma}^b \\ k_{NI}^b & k_{NN}^b & 0 \\ k_{\gamma I}^b & 0 & k_{\gamma\gamma}^b \end{bmatrix}$$

$$x_D = \begin{Bmatrix} x_\gamma^d \\ x_O \end{Bmatrix}, K_d = \begin{bmatrix} k_{\gamma\gamma}^d & k_{\gamma O}^d \\ k_{O\gamma}^d & k_{OO}^d \end{bmatrix} \quad (1)$$

where x_γ^b and x_γ^d correspond to interface DOFs of the blade and the disk, respectively, x_N represents contact nonlinear DOFs of the blade (e.g. contact nodes at shrouds), x_I represents remaining interior DOFs of the blade and x_O corresponds to other DOFs of the disk except interface DOFs. Note that in more general context, x_N could represent any group of active DOFs that are retained during CB-CMS reduction. Throughout this study, all mass matrices are partitioned exactly in the same way as their corresponding stiffness matrices.

2.2 Blade component reduction (Based on CB-CMS)

In order to apply CB-CMS on the blade component, blade DOFs are grouped into x_m and x_s vectors to separate master (physical retained) and slave DOFs. Master DOFs include interface DOFs x_γ^b, necessary to enforce CMS primal assembly and nonlinear DOFs x_N, retained for the nonlinear forced response computations. The partitioned blade displacement vector and the corresponding stiffness matrix, take the following form:

$$x_B = \begin{Bmatrix} x_I \\ \hline x_N \\ x_\gamma^b \end{Bmatrix} = \begin{Bmatrix} x_s \\ x_m \end{Bmatrix}$$

$$K_b = \begin{bmatrix} k_{ss} & k_{sm} \\ k_{ms} & k_{mm} \end{bmatrix} = \left[\begin{array}{c|cc} k_{II}^b & k_{IN}^b & k_{I\gamma}^b \\ \hline k_{NI}^b & k_{NN}^b & 0 \\ k_{\gamma I}^b & 0 & k_{\gamma\gamma}^b \end{array}\right] \tag{2}$$

The blade DOFs can now be reduced using the CB-CMS transformation matrix R_{cb}, as follows:

$$\begin{Bmatrix} x_s \\ x_m \end{Bmatrix} = R_{cb} \begin{Bmatrix} \eta \\ x_m \end{Bmatrix}, R_{cb} = \begin{bmatrix} \Phi_f & \Psi_c \\ 0 & I \end{bmatrix} \tag{3}$$

where Φ_f are fixed-interface modeshapes of the blade constrained at its master DOFs and $\Psi_c = -k_{ss}^{-1} k_{sm}$ are static constraint modes. Projecting the blade structural matrices onto the CB-CMS coordinates, yields:

$$K_{CB} = R_{CB}^T K_b R_{CB} = \begin{bmatrix} \Lambda_i^b & 0 \\ 0 & K_{cb}^b \end{bmatrix}$$
$$M_{CB} = R_{CB}^T M_b R_{CB} = \begin{bmatrix} I & m_{\eta m} \\ m_{m\eta} & M_{cb}^b \end{bmatrix} \tag{4}$$

where K_{CB} and M_{CB} are blade CB-CMS reduced stiffness and mass matrices, respectively. Different partitions of K_{CB} and M_{CB} are given below:

$$K_{cb}^b = k_{mm} - k_{ms} k_{ss}^{-1} k_{sm}$$
$$\Lambda_i^b = \Phi_f^T k_{ss} \Phi_f$$
$$M_{cb}^b = m_{mm} + \Psi_c^T m_{ss} \Psi_c + m_{ms} \Psi_c + \Psi_c^T m_{sm}$$
$$M_{\eta m} = \Phi_f^T m_{ss} \Psi_c + \Phi_f^T m_{sm} \tag{5}$$

Note that the lower right partition of K_{CB} represents the blade CB-CMS reduced stiffness matrix corresponding to retained physical DOFs (i.e. blade nonlinear and interface DOFs) and is expanded as follows:

$$K_{cb}^{b}=\begin{bmatrix} k_{cb,NN}^{b} & k_{cb,N\gamma}^{b} \\ k_{cb,\gamma N}^{b} & k_{cb,\gamma\gamma}^{b} \end{bmatrix}=\begin{bmatrix} k_{NN}^{b}-k_{NI}^{b}k_{II}^{b^{-1}}k_{IN}^{b} & -k_{NI}^{b}k_{II}^{b^{-1}}k_{I\gamma}^{b} \\ -k_{\gamma I}^{b}k_{II}^{b^{-1}}k_{IN}^{b} & k_{\gamma\gamma}^{b}-k_{\gamma I}^{b}k_{II}^{b^{-1}}k_{I\gamma}^{b} \end{bmatrix} \tag{6}$$

Different partitions of M_{CB} are presented in Appendix B.

2.3 Interface and disk reduction (Based on loaded interface modeshapes)

The proposed modal reduction operates on the disk DOFs plus the interface DOFs retained during the blade CB-CMS reduction, by projecting them to a set of generalized coordinates. Loaded interface modeshapes of the disk are obtained by statically condensing the blade interior DOFs on blade-disk interface DOFs x_{γ}^{b} and then solving the eigenvalue problem of the loaded disk system. Static condensation of interior blade DOFs on interface DOFs can be obtained by:

$$x_B=\begin{Bmatrix} x_I \\ x_N \\ \hdashline x_{\gamma}^{b} \end{Bmatrix}=\begin{Bmatrix} x_i^{b} \\ x_{\gamma}^{b} \end{Bmatrix}=\begin{bmatrix} \psi_c^{b} \\ I \end{bmatrix}x_{\gamma}^{b}=\beta x_{\gamma}^{b} \tag{7}$$

where x_i^{b} are interior DOFs of the blade and ψ_c^{b} are static constraint modes, given by:

$$\psi_c^{b}=-k_{ii}^{-1}k_{i\gamma}=-\begin{bmatrix} k_{II}^{b} & k_{IN}^{b} \\ k_{NI}^{b} & k_{NN}^{b} \end{bmatrix}^{-1}\begin{bmatrix} k_{I\gamma}^{b} \\ 0 \end{bmatrix} \tag{8}$$

Note that, in contrast to the blade CB-CMS reduction where both x_N and x_{γ}^{b} DOFs are retained as master DOFs, here, the blade DOFs are statically condensed only on interface DOFs x_{γ}^{b} and thus the ψ_c^{b} matrix includes the constraint modes of the cantilevered blade. The Guyan reduced mass and stiffness matrices of the blade can be obtained by:

$$\begin{aligned} k_{Guyan}^{b}&=\psi_c^{bT}K_b\psi_c^{b}=k_{\gamma\gamma}^{b}-k_{\gamma i}k_{ii}^{-1}k_{i\gamma} \\ m_{Guyan}^{b}&=\psi_c^{bT}M_b\psi_c^{b}=m_{\gamma\gamma}^{b}+\psi_c^{bT}M_{ii}\psi_c^{b}+M_{\gamma i}\psi_c^{b}+\psi_c^{bT}M_{i\gamma} \end{aligned} \tag{9}$$

As a final step, the mass and stiffness matrices of the loaded disk are obtained:

$$\tilde{K} = \begin{bmatrix} k^d_{\gamma\gamma} + k^b_{Guyan} & k^d_{\gamma O} \\ k^d_{O\gamma} & k^d_{OO} \end{bmatrix}$$
$$\tilde{M} = \begin{bmatrix} m^d_{\gamma\gamma} + m^b_{Guyan} & m^d_{\gamma O} \\ m^d_{O\gamma} & m^d_{OO} \end{bmatrix} \tag{10}$$

Solving the following eigenvalue problem:

$$\left(\tilde{K} - \Lambda_{LI}\tilde{M}\right)\tilde{\varphi} = 0 \tag{11}$$

gives the disk loaded interface modeshapes $\tilde{\varphi}$ and eigenvalues Λ_{LI}. Prior to applying the interface-disk modal reduction, one should perform a CMS assembly to cast the partially reduced blisk structural matrices. Enforcing interface compatibility between the CB-CMS reduced blade and the disk component, yields:

$$K_1 = \begin{bmatrix} \Lambda^b_i & 0 & 0 & 0 \\ 0 & k^b_{cb,NN} & k^b_{cb,N\gamma} & 0 \\ 0 & k^b_{cb,\gamma N} & \boxed{k^b_{cb,\gamma\gamma} + k^d_{\gamma\gamma}} & k^d_{\gamma O} \\ 0 & 0 & k^d_{O\gamma} & k^d_{OO} \end{bmatrix}$$
$$M_1 = \begin{bmatrix} I & m_{\eta N} & m_{\eta\gamma} & 0 \\ m_{N\eta} & m^b_{cb,NN} & m^b_{cb,N\gamma} & 0 \\ m_{\gamma\eta} & m^b_{cb,\gamma N} & \boxed{m^b_{cb,\gamma\gamma} + m^d_{\gamma\gamma}} & m^d_{\gamma O} \\ 0 & 0 & m^d_{O\gamma} & m^d_{OO} \end{bmatrix} \tag{12}$$

where the dashed rectangles highlight the blade-disk interface portion. Now, the further reduction can be achieved by expressing the interface and disk DOFs of the displacement vector in terms of loaded interface modal coordinates:

$$\begin{Bmatrix} \eta \\ x_N \\ x_\gamma \\ x_O \end{Bmatrix} = \begin{bmatrix} I & 0 & 0 \\ 0 & I & 0 \\ 0 & 0 & \tilde{\varphi} \end{bmatrix} \begin{Bmatrix} \eta \\ x_N \\ \tilde{\eta} \end{Bmatrix} = R_{LI} \begin{Bmatrix} \eta \\ x_N \\ \tilde{\eta} \end{Bmatrix} \tag{13}$$

where R_{LI} denotes the LI reduction matrix. The final reduced mass and stiffness matrices of the fundamental sector is obtained by implementing the following projections:

$$K_{rom} = R_{LI}^T K_1 R_{LI}$$
$$M_{rom} = R_{LI}^T M_1 R_{LI}$$

(14)

Final reduced stiffness matrix and its different partitions take the following form:

$$K_{rom} = \left[\begin{array}{cc:c} I & 0 & 0 \\ 0 & I & 0 \\ \hdashline 0 & 0 & \begin{bmatrix}\tilde{\varphi}_\gamma \\ \tilde{\varphi}_O\end{bmatrix} \end{array}\right]^T \left[\begin{array}{c:cc} \Lambda_i^b & 0 & 0 \\ \hdashline 0 & k_{cb,NN}^b & k_{cb,N\gamma}^b \\ 0 & k_{cb,\gamma N}^b & k_{cb,\gamma\gamma}^b + k_{\gamma\gamma}^d \quad k_{\gamma O}^d \\ 0 & 0 & k_{O\gamma}^d \quad k_{OO}^d \end{array}\right] \left[\begin{array}{cc:c} I & 0 & 0 \\ 0 & I & 0 \\ \hdashline 0 & 0 & \begin{bmatrix}\tilde{\varphi}_\gamma \\ \tilde{\varphi}_O\end{bmatrix} \end{array}\right]$$
$$= \begin{bmatrix} \Lambda_i^b & 0 & 0 \\ 0 & k_{cb,NN}^b & k_{cb,N\gamma}^b \tilde{\varphi}_\gamma \\ 0 & \tilde{\varphi}_\gamma^T k_{cb,\gamma N}^b & [\hat{k}] \end{bmatrix}$$

(15)

where

$$\hat{k} = \begin{bmatrix}\tilde{\varphi}_\gamma \\ \tilde{\varphi}_O\end{bmatrix}^T \begin{bmatrix} k_{cb,\gamma\gamma}^b + k_{\gamma\gamma}^d & k_{\gamma O}^d \\ k_{O\gamma}^d & k_{OO}^d \end{bmatrix} \begin{bmatrix}\tilde{\varphi}_\gamma \\ \tilde{\varphi}_O\end{bmatrix}.$$

(16)

The evolution of the original set of DOFs of the fundamental sector during the reduction is depicted in Fig. 1.

$$\begin{Bmatrix} x_I \\ x_N \\ x_\gamma \\ x_O \end{Bmatrix} = \begin{Bmatrix} x_s = x_I \\ x_m = \begin{bmatrix} x_N \\ x_\gamma \end{bmatrix} \\ x_O \end{Bmatrix} \xrightarrow[\text{Blade Component}]{R_{CB}} \begin{Bmatrix} \eta \\ x_m \\ x_O \end{Bmatrix}$$
$$\begin{Bmatrix} \eta \\ x_m \\ x_O \end{Bmatrix} = \begin{Bmatrix} \eta \\ x_m = \begin{bmatrix} x_N \\ x_\gamma \end{bmatrix} \\ x_O \end{Bmatrix} \xrightarrow[\text{Interface-Disk Component}]{R_{LI}} \begin{Bmatrix} \eta \\ x_N \\ \tilde{\eta} \end{Bmatrix}$$

Fig. 1 Evolution of DOFs during the reduction

2.4 Full bladed disk ROM

Without losing any generality of the presented formulation for the single sector, this reduction approach can be easily extended to the full system. In this case, each partition of matrices in Eqn. (1) should be replaced by a block diagonal matrix, representing the contribution of all sectors in the

structural matrices. Accordingly, the blade and the disk stiffness matrices of the full structure can be expressed as follows:

$$K_B = \begin{bmatrix} I \otimes k_{II}^b & I \otimes k_{IN}^b & I \otimes k_{I\gamma}^b \\ I \otimes k_{NI}^b & I \otimes k_{NN}^b & 0 \\ I \otimes k_{\gamma I}^b & 0 & I \otimes k_{\gamma\gamma}^b \end{bmatrix}$$

$$K_D = \begin{bmatrix} I \otimes k_{\gamma\gamma}^d & I \otimes k_{\gamma O}^d \\ I \otimes k_{O\gamma}^d & \bar{k}_{OO}^d \end{bmatrix} \tag{17}$$

where *I* is an identity matrix of size *N* (number of blades) and ⊗ denotes the Kronecker product. In Eqn. (17), $\bar{k}_{OO}^d$ is the partition of the full disk component corresponding to x_O DOFs. Note that $\bar{k}_{OO}^d$ is not a pure block diagonal partition, due to the presence of internal interfaces between disk sectors. Since the blades are uncoupled to each other, the CB-CMS transformation matrix of *N*-blades structure, can be obtained from the single blade transformation matrix, as follows:

$$\bar{R}_{cb} = \begin{bmatrix} I \otimes \Phi_f & I \otimes \Psi_c \\ 0 & I \end{bmatrix} \tag{18}$$

Note that, no mistuning is introduced yet and blades are identical. The CB-CMS reduced stiffness matrix of the full set of blades, can be described as:

$$\bar{K}_{CB} = \begin{bmatrix} I \otimes \Lambda_i^b & 0 & 0 \\ 0 & I \otimes k_{cb,NN}^b & I \otimes k_{cb,N\gamma}^b \\ 0 & I \otimes k_{cb,\gamma N}^b & I \otimes k_{cb,\gamma\gamma}^b \end{bmatrix} \tag{19}$$

Enforcing the interface compatibility over the interface DOFs, yields an assembly composed of CB-CMS reduced blades attached to the full disk at the blade-disk interfaces. The stiffness matrix of this partially reduced system is expressed as:

$$K_I = \begin{bmatrix} I \otimes \Lambda_i^b & 0 & 0 & 0 \\ 0 & I \otimes k_{cb,NN}^b & I \otimes k_{cb,N\gamma}^b & 0 \\ 0 & I \otimes k_{cb,\gamma N}^b & I \otimes k_{\gamma\gamma}^{rom} & I \otimes k_{\gamma O}^d \\ 0 & 0 & I \otimes k_{O\gamma}^d & \bar{k}_{OO}^d \end{bmatrix} \tag{20}$$

where $k_{\gamma\gamma}^{rom} = k_{cb,\gamma\gamma}^b + k_{\gamma\gamma}^d$ denotes the interface stiffness partition, made of the CB-CMS reduced stiffness of the blade interface added to the interface stiffness of the disk component. The K_I matrix must be now further reduced by means of loaded interface modeshapes of the full disk (i.e. $\widetilde{\Phi}$). Due to the cyclic symmetry of the system, modeshapes of the full disk can be obtained by expanding modeshapes of the loaded fundamental sector computed with cyclic symmetry boundary conditions [28]. The final reduced stiffness matrix of the tuned bladed disk is:

$$K_{ROM} = \begin{bmatrix} I \otimes \Lambda_i^b & 0 & 0 \\ 0 & I \otimes k_{cb,NN}^b & \left(I \otimes k_{cb,N\gamma}^b\right)\tilde{\Phi}_\gamma \\ 0 & \tilde{\Phi}_\gamma^T\left(I \otimes k_{cb,\gamma N}^b\right) & [\hat{K}] \end{bmatrix} \tag{21}$$

with

$$\hat{K} = \begin{bmatrix} \tilde{\Phi}_\gamma \\ \tilde{\Phi}_O \end{bmatrix}^T \begin{bmatrix} \underset{n=1..N}{Bdiag}[k_{\gamma\gamma}^{rom^{(n)}}] & I \otimes k_{\gamma O}^d \\ I \otimes k_{O\gamma}^d & \bar{k}_{OO}^d \end{bmatrix} \begin{bmatrix} \tilde{\Phi}_\gamma \\ \tilde{\Phi}_O \end{bmatrix} \tag{22}$$

where $\underset{n=1..N}{Bdiag}[k_{\gamma\gamma}^{rom^{(n)}}] = I \otimes k_{\gamma\gamma}^{rom}$.

Note that, the same discussion and methodology is used to obtain the reduced mass matrix of the full system i.e. M_{ROM} (a detailed description is given in Appendix B).

2.5 Mistuning Modeling

The presented novel reduction technique is tailored for small blade mistuning. Accordingly, the disk is treated as a tuned cyclic structure and mistuning is introduced as variations in Young's modulus of blades (blade frequency mistuning). In order to introduce mistuning to the final reduced model; in terms of Young's modulus variation of blades; it is beneficial to recall that based on the Hooke's law

for isotropic materials, the element stiffness matrix k^e which relates nodal forces to nodal displacements, is linearly dependent to Young's modulus as follows:

$$k^e = E \cdot k^{e\prime} \tag{23}$$

As described before, the CB-CMS method is used to reduce the blades. Therefore, the effect of blade Young's modulus variation on the CB-CMS reduction matrix R_{cb}, defined by Eqn. (3), is investigated. It turns out that for a single component of nominal Young's modulus *E*, the corresponding CB-CMS transformation matrix is invariant of Young's modulus, and the resultant CB-CMS reduced stiffness matrix is linearly dependent to *E* as follows:

$$K_{CB} = \begin{bmatrix} E \cdot \Lambda_i'^b & 0 \\ 0 & E \cdot \left(k'_{mm} - k'_{ms} k'^{-1}_{ss} k'_{sm} \right) \end{bmatrix} \tag{24}$$

In the case of mistuned systems, the random Young's modulus can be defined as:

$$E_n = E \cdot \left(1 + \delta_n\right) \tag{25}$$

where E_n is the Young's modulus of the *n*th blade, *E* is the nominal Young's modulus and δ_n is a non-dimensional mistuning parameter used to perturb *E*. Accordingly, one may obtain the final reduced form of the mistuned stiffness matrix as follows:

$$K_{ROM} = \begin{bmatrix} \underset{n=1..N}{diag}\ (1+\delta_n) \otimes \Lambda_i^b & 0 & 0 \\ 0 & \underset{n=1..N}{diag}\ (1+\delta_n) \otimes k^b_{cb,NN} & \left(\underset{n=1..N}{diag}\ (1+\delta_n) \otimes k^b_{cb,N\gamma} \right) \tilde{\Phi}_\gamma \\ 0 & \tilde{\Phi}_\gamma^T \left(\underset{n=1..N}{diag}\ (1+\delta_n) \otimes k^b_{cb,\gamma N} \right) & [\hat{K}] \end{bmatrix} \tag{26}$$

with

$$\hat{K} = \begin{bmatrix} \tilde{\Phi}_\gamma \\ \tilde{\Phi}_O \end{bmatrix}^T \begin{bmatrix} \underset{n=1..N}{Bdiag}[k_{\gamma\gamma}^{*rom^{(n)}}] & I \otimes k^d_{\gamma O} \\ I \otimes k^d_{O\gamma} & \bar{k}^d_{OO} \end{bmatrix} \begin{bmatrix} \tilde{\Phi}_\gamma \\ \tilde{\Phi}_O \end{bmatrix} \tag{27}$$

where

$$\underset{n=1..N}{Bdiag}\,[k_{\gamma\gamma}^{*rom(n)}] = \underset{n=1..N}{Bdiag}\,[k_{cb,\gamma\gamma}^{*b(n)}] + \underset{n=1..N}{Bdiag}\,[k_{\gamma\gamma}^{d(n)}] = \underset{n=1..N}{diag}\,(1+\delta_n)\otimes k_{cb,\gamma\gamma}^{b} + I \otimes k_{\gamma\gamma}^{d}\,. \tag{28}$$

Note that superscript $(.)^*$; first introduced in Eqn. (27); will be used to denote a mistuned partition. For ROMs to be useful in stochastic nonlinear analysis, necessary to assess statistically the effect of mistuning on the response level of the blades, direct introduction of mistuning in the final ROM is necessary to prevent multiple reductions, one per each analyzed mistuning pattern. K_{ROM} as formulated in Eqn. (26), allows for direct introduction of mistuning in all its blocks except for $\widehat{K}$, which depends on all random variables δ_n and needs to be recomputed for each mistuning pattern. In order to overcome this issue, one option is to assume that the blade mistuning has a negligible effect on this partition and $\widehat{K}$ remains constant regardless of the mistuning pattern. It is worth mentioning that, the interface portion of the blade CB-CMS stiffness matrix (i.e. $k_{cb,\gamma\gamma}^{*b^{(n)}}$) is the only source of mistuning introduced in $\widehat{K}$, as a byproduct of CMS assembly. From physical point of view, assuming a constant $\widehat{K}$ matrix is equivalent to neglect the effect of mistuning on a portion of constraint modes corresponding to interface DOFs of the blades. The validity of this assumption is discussed in the result section.

Another option is to efficiently compute $\widehat{K}$ without neglecting the effect of mistuning on this partition. This alternative solution requires a special treatment. To this end, an exact solution is developed based on sector level computations and modeshapes that have already been computed during the reduction steps. The alternative method is illustrated in the next section.

It is worth mentioning that the interface-disk reduction approach is based on loaded interface modeshapes of the disk. As discussed in Interface-Disk reduction section, loaded interface modeshapes are obtained by adding Guyan reduced matrices of the tuned blades to the interface partition of the disk matrices and solving the eigenvalue problem of the loaded disk system. In fact the loaded interface modeshapes obtained in the reduction approach are calculated by statically condensing the tuned blades onto the blade-disk interfaces. However, in the reduction process of a mistuned system, one may consider the effect of blade mistuning on the loaded interface modeshapes

of the disk. In this context, mistuned loaded interface modeshapes refer to those modeshapes that are calculated by condensing the mistuned blades onto the blade-disk interfaces. Note that, neglecting the effect of mistuning on loaded interface modeshapes of the disk could be a valid assumption. Since, the dominant portion of $\widetilde{K}$ is composed of the tuned disk stiffness matrix, the added mistuned portion (i.e. Guyan stiffness of mistuned blades $\underset{n=1..N}{Bdiag}[k_{Guyan}^{*b^{(n)}}] = \underset{n=1..N}{diag}(1+\delta_n) \otimes k_{Guyan}^{b}$) to the interface DOFs could not considerably change the modeshapes of the full disk. Therefore, it is predictable that neglecting the effects of mistuning only on Guyan stiffness of the blades, provides acceptable accuracy. The validity of this assumption is discussed later in the result section.

2.6 Sector level computations (requisites)

As it is seen in Eqn. (26) all partitions of K_{ROM} are linearly dependent to mistuning parameters except for its extreme lower right partition $\widehat{K}$, which is dependent to all random parameters δ_n. Thus, to take into account the effect of mistuning on this partition, one should compute $\widehat{K}$ for each mistuning pattern. This would be cumbersome for statistical analyses. Moreover, all other partitions of K_{ROM} are constructed from a single sector stiffness matrix and cyclic loaded interface modes of the disk. However, in industrial applications, projecting the full disk matrix onto the cyclic loaded interface modeshapes seems impractical or even impossible. Therefore, an alternative way for computation of $\widehat{K}$ based on sector level computations is needed. For simplicity of notation the following operator is defined as:

$$blkdg[.] = \underset{n=1..N}{Bdiag}[.] \oplus 0_k = \begin{pmatrix} \underset{n=1..N}{Bdiag}[.] & 0 & \cdots & 0 \\ 0 & \begin{pmatrix} 0 & \cdots & 0 \\ \vdots & \ddots & \vdots \\ 0 & \cdots & 0 \end{pmatrix}_{k\times k} \\ \vdots & \\ 0 & \end{pmatrix} \tag{29}$$

where 0_k denotes additive identity in *k* (*k* by *k* null matrix) and $\oplus$ denotes direct sum of matrices which is defined in Appendix A. This operator will be used to denote; in a compact way; a block diagonal matrix of size equal to the total number of disk DOFs with all entries equal to zero except for

the partition corresponding to the blade-disk interface DOFs. By introducing Eqn. (29) into the loaded disk stiffness matrix which is composed of the disk stiffness matrix K_D (defined by Eqn. (17)) and the Guyan-reduced stiffness matrices of the blades added to the blade-disk interfaces, it can be represented in the following compact way:

$$\tilde{K} = \begin{bmatrix} I \otimes k^d_{\gamma\gamma} + \underset{n=1..N}{Bdiag}\,[k^{b(n)}_{Guyan}] & I \otimes k^d_{\gamma O} \\ I \otimes k^d_{O\gamma} & \bar{k}^d_{OO} \end{bmatrix} = K_D + blkdg[k^b_{Guyan}] \tag{30}$$

By substituting Eqn. (17) into Eqn. (27) and using the compact notation defined by Eqn. (29), $\hat{K}$ can be written as:

$$\begin{aligned} \hat{K} &= \tilde{\Phi}^T \begin{pmatrix} \underset{n=1..N}{Bdiag}[k^{*rom^{(n)}}_{\gamma\gamma}] & I \otimes k^d_{\gamma O} \\ I \otimes k^d_{O\gamma} & \bar{k}^d_{OO} \end{pmatrix} \tilde{\Phi} = \tilde{\Phi}^T \begin{pmatrix} \underset{n=1..N}{Bdiag}[K^{*b^{(n)}}_{cb,\gamma\gamma}] + I \otimes k^d_{\gamma\gamma} & I \otimes k^d_{\gamma O} \\ I \otimes k^d_{O\gamma} & \bar{k}^d_{OO} \end{pmatrix} \tilde{\Phi} \\ &= \tilde{\Phi}^T \left(K_D + blkdg[k^{*b}_{cb,\gamma\gamma}] \right) \tilde{\Phi} \end{aligned} \tag{31}$$

As previously stated, $\hat{K}$ is composed of tuned disk stiffness matrix and mistuned CB-CMS stiffness of blade interfaces. By adding and subtracting the Guyan stiffness matrix of the tuned blades to the interface DOFs of the $\hat{K}$ central core and using Eqn. (30), one may cast $\hat{K}$ as follows:

$$\hat{K} = \tilde{\Phi}^T \begin{pmatrix} K_D + blkdg[k^b_{Guyan}] - blkdg[k^b_{Guyan}] \\ + blkdg[k^{*b}_{cb,\gamma\gamma}] \end{pmatrix} \tilde{\Phi} = \tilde{\Phi}^T \left(\tilde{K} - blkdg[k^b_{Guyan}] + blkdg[k^{*b}_{cb,\gamma\gamma}] \right) \tilde{\Phi}$$

$$= \begin{Bmatrix} diag\left(\Lambda_{LI}\right) - \tilde{\Phi}^T_{\gamma} \underset{n=1..N}{Bdiag}\,[k^{b(n)}_{Guyan}] \tilde{\Phi}_{\gamma} \\ + \tilde{\Phi}^T_{\gamma} \underset{n=1..N}{Bdiag}\,[k^{*b(n)}_{cb,\gamma\gamma}] \tilde{\Phi}_{\gamma} \end{Bmatrix} \tag{32}$$

Now, based on the derived formulation, $\hat{K}$ can be computed using sector level calculations. According to Eqn. (32), $\hat{K}$ is mainly constructed from the terms that are independent to mistuning (i.e. the first two terms of Eqn. (32)) and are just computed for once. In addition, the mistuning is introduced (i.e. the third term of Eqn. (32)) by projecting a sparse matrix onto the interface portion of loaded interface

modeshapes. All those mentioned above, make the alternative formulation computationally cheap and suitable for statistical analyses.

3 Numerical Solution

The reduced equations of motion of the system can be written as:

$$M_{rom}\ddot{x}_r(t) + C_{rom}\dot{x}_r(t) + K_{rom}x_r(t) = F_{nl}(x_r(t), \dot{x}_r(t)) + F_{ex}(t) \tag{33}$$

where $x_r(t)$ is the displacement vector of the final reduced system comprised of nonlinear contact DOFs and CB and LI generalized coordinates. M_{rom}, C_{rom} and K_{rom} are mass, damping and stiffness matrices of the final reduced system, respectively. F_{nl} is the vector of nonlinear contact forces and it depends on relative displacements of contact nodes. F_{ex} is the vector of the external forces applied on the system. Note that, the reduced damping matrix C_{rom} can be computed in a systematic manner using the proposed reduction technique. However, by assuming a proportional damping for the ROM, C_{rom} matrix can be simply constructed from reduced mass and stiffness matrices. Based on the multi-harmonic balance method [4], one may approximate the displacements and the forces as follows:

$$\begin{aligned} x_r(t) &\approx x_r^0 + \mathrm{Re}\left(\sum_{h=1..H} \bar{X}_r^{(h)} e^{ih\omega t} \right) \\ F_{nl}(t) &\approx F_{nl}^0 + \mathrm{Re}\left(\sum_{h=1..H} \bar{F}_N^{(h)} e^{ih\omega t} \right) \\ F_{ex}(t) &\approx F_{ex}^0 + \mathrm{Re}\left(\sum_{h=1..H} \bar{F}_E^{(h)} e^{ih\omega t} \right) \end{aligned} \tag{34}$$

where x_r^0, F_{nl}^0 and F_{ex}^0 represent static equilibrium solutions, static external forces (e.g. centrifugal forces) and static contact forces, respectively. H denotes the number of considered harmonics and ω is the frequency of the excitation force. Also, Re indicates the real part of complex valued functions. Substituting Eqn. (34) into Eqn. (33) yields the following algebraic balance equations for each harmonic h:

$$[-(h\omega)^2 M_{rom} + ih\omega C_{rom} + K_{rom}]^{(h)} - \bar{F}_N^{(h)} - \bar{F}_E^{(h)} = 0 \tag{35}$$

An iterative approach based on AFT logic [26] is used to solve the nonlinear equations of Eqn. (35), where the nonlinear contact forces are modeled by means of node-to-node state-of-the-art contact elements ([27]).

3.1 FE model

The considered test case in this study is a simplified turbine bladed disk with 12 blades developed in ANSYS. The single sector model contains 429 elements and 460 nodes and the full model comprises 11429 nodes and 34,287 DOFs in total. The FE model of the academic bladed disk and a single sector model are depicted in Fig. 2.

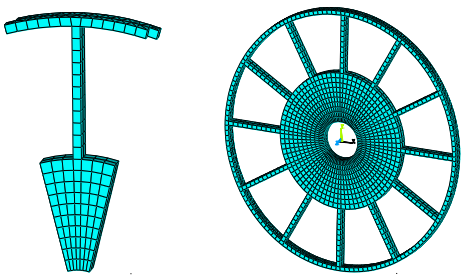

Fig. 2 FE model of the academic bladed disk and the single sector model

The bladed disk is fixed at two circular rows of node lying on the outer faces of the disk. In the fundamental sector, each contact surface at the shroud comprises 4 nonlinear contact nodes and also the blade-disk interface contains 6 nodes. All the linear analyses (e.g. natural frequencies, modeshapes and etc.) are performed on a blisk in fully stick condition, in order to have boundary conditions at shroud interfaces more similar to microslip condition, which are typical operating conditions for shrouds. Fully stick condition is modeled by merging contact node pairs at adjacent shrouds.

Natural frequencies versus the number of nodal diameters (NDs) for the tuned bladed disk in stick condition is depicted in Fig. 3.

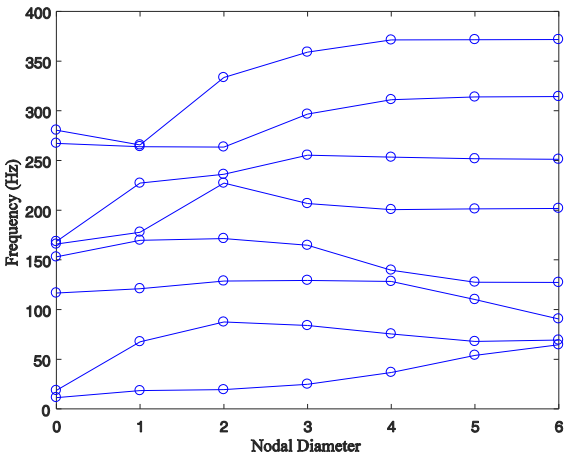

Fig. 3 Natural frequency versus nodal diameters for the tuned bladed disk in fully stick condition

This plot reveals underlying characteristics of system dynamics such as frequency veerings and disk/blade dominated modeshapes. In frequency veering regions blade and disk dominated modeshapes veer from each other by further increasing the ND. Note that, since the adjacent blades are coupled at the shrouds, blade dominated modes are not pure horizontal lines and a slight softening/stiffening behavior is seen for blade mode families. In fact, in some frequency ranges, the vibrational motion of the coupled shrouds (which resemble a ring component attached to the blade tips) has a dominant out of plane component along axial direction. This will introduce an additional compliance to the system. In contrary, increasing the ND in some other ranges, results in a circumferential mode of the coupled shrouds (in tangential direction), which will decrease the system compliance. In Fig. 3, slanted lines could also be representative of inter-blade couplings which makes it more difficult to distinguish them from disk dominated modes.

3.2 Results for linear tuned bladed disk

In order to evaluate the accuracy of the proposed reduction technique, eigenvalues of the final reduced system are compared with the exact eigenvalues of the full FE model, obtained in ANSYS. The

eigenvalue deviation is defined as $(\lambda_{ROM} - \lambda_{Full})/\lambda_{Full}$ where λ_{ROM} denotes eigenvalues of the reduced system and λ_{Full} denotes exact eigenvalues of the full model. Here, the first 100 natural frequencies of the tuned system are compared. Since, the reduction is based on two distinct sets of component modes, the number of retained modes of each set, defines the accuracy of the final ROM. Here, number of retained modes is selected based on the convergence analysis. This is a preliminary step, especially for nonlinear analyses, since, the contribution of higher modes or the presence of modal interaction in the system, are not known a priori. In addition, "the frequency range of interest" should be taken into account. For instance, near the blade dominated modeshapes, increasing the number of retained loaded interface modeshapes (which are representative of disk dynamics) beyond a certain limit, does not enhance the accuracy of the ROM. In all results, the indicated number of CB modes, refers to the full system and not the retained modes per blade.

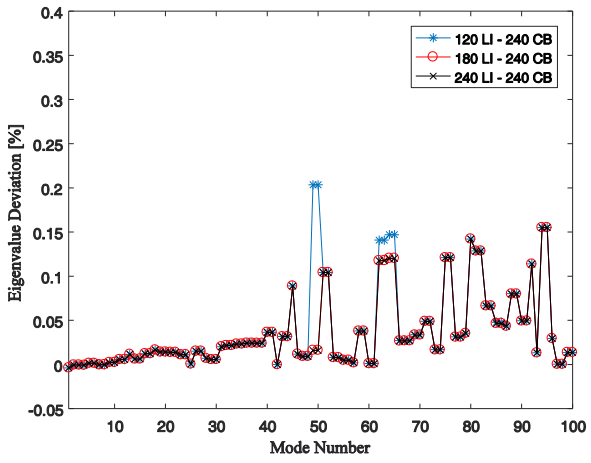

Fig. 4 The influence of loaded interface (LI) modeshapes on the eigenvalue deviation between ROM and ANSYS results (tuned blisk in stick)

The effect of retained loaded interface modeshapes in the ROM on the accuracy of the computed eigenvalues is shown in Fig. 4. As it is seen, increasing the number of loaded interface modes in the ROM, increases the accuracy up to a certain level. From a certain level, adding extra modeshapes (corresponding to higher frequencies) does not contribute to the accuracy of the results in the studied range (first 100 modes).

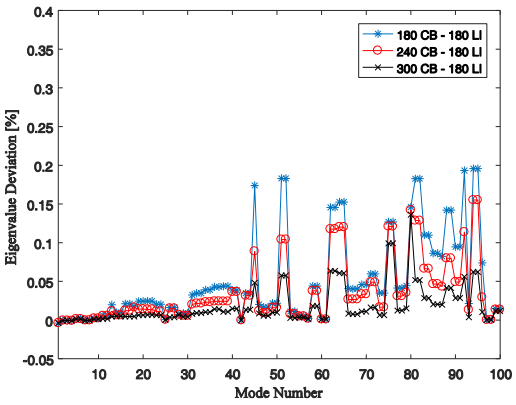

Fig. 5 The influence of CB modes on the eigenvalue deviation between ROM and ANSYS results (tuned blisk in stick)

Figure 5 shows the influence of the CB modes used in the ROM, on the accuracy of the computed eigenvalues. The number of CB modes used in the ROM can considerably affect the accuracy of the results. It should be noted that the real boundary conditions at the shrouds are different with the CB-CMS boundary conditions where blades are clamped at interface and nonlinear contact nodes. Thus, increasing the number of retained CB modes, will increase the accuracy more significantly. These results, reveal the capability of proposed reduction technique in accurately predicting the natural frequencies of the system.

3.3 Results for linear mistuned bladed disk

The performance of the proposed ROM in predicting the eigenvalues of a mistuned blisk is assessed here. The mistuned bladed disk model is obtained by varying the blades Young's modulus (3%) from its nominal value. The random mistuning pattern considered for the test case is listed in Table. 1.

The influence of the number of LI and CB modes used in the ROM on the eigenvalue deviations is illustrated in Figs. 6 and 7, respectively.

Table 1. Blade frequency mistuning pattern

Blade Number	Mistuning Parameter δ_n
1	0
2	0.0114
3	0.0149
4	-0.0030
5	-0.0250
6	-0.0163
7	0.0248
8	-0.0209
9	0.0195
10	0.0023
11	0.0298
12	-0.0253

As can be observed, similar to the case of tuned blisk, increasing the number of retained modes enhances the results by decreasing the deviation from the exact eigenvalues obtained in ANSYS.

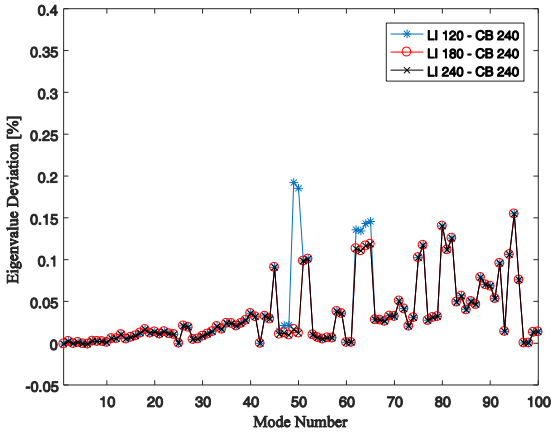

Fig. 6 The influence of loaded interface (LI) modeshapes on the eigenvalue deviation between ROM and ANSYS results (mistuned blisk in stick)

Figures 6 and 7, demonstrate the high accuracy of the reduction approach in predicting the eigenvalues of the mistuned model. Note that sufficient number of LI and CB modes should be retained in the ROM to achieve acceptable accuracy. For instance, the maximum error for predicted eigenvalue of the mistuned system; obtained from a ROM containing 300 CB and 180 loaded interface modes; is about 0.137 %.

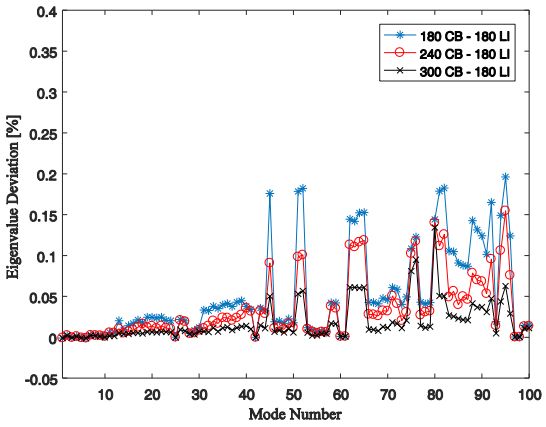

Fig. 7 The influence of CB modes on the eigenvalue deviation between ROM and ANSYS results (mistuned blisk in stick)

3.4 Results based on mistuned loaded interface modeshapes

The effect of mistuned loaded interface modeshapes on the performance of the ROM is investigated. Figure 8 shows the accuracy of two ROMs (based on tuned and mistuned loaded interface modeshapes), in predicting the natural frequencies of the mistuned bladed disk.

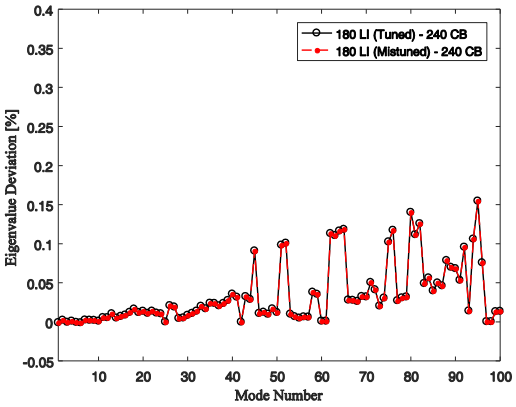

Fig. 8 The effect of mistuned loaded interface (LI) modeshapes on the accuracy of the predicted eigenvalues by the ROM

As can be seen results coincide well for both ROMs. In other words, considering mistuned loaded interface modeshapes as the reduction basis does not improve the accuracy of the ROM. The demonstrated results are of great importance, especially for statistical analyses, since, changing and computing the reduction basis for each mistuning pattern is not practical. In addition the tuned and

mistuned loaded interface modeshapes are compared with each other using the modal assurance criterion (MAC).

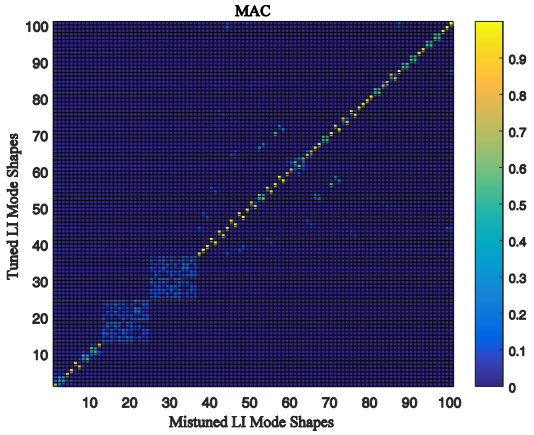

Fig. 9 Modal correlation between tuned and mistuned loaded interface (LI) modeshapes

Figure 9 shows a comparison between the tuned and the mistuned loaded interface modeshapes. As it is seen, most part of the MAC diagonal is almost unity indicating that the modeshapes are similar. However, a weak correlation is seen between two dozen modes (i.e. 13-24 and 25-36). Note that the MAC matrix has a block diagonal structure in this range. So, any modeshape chosen from either of these two sets, has modal properties similar to that of modes lying in the same set and is orthogonal to all other modes. For instance, the mistuned loaded interface modeshape number 15 can be represented as a linear combination of tuned loaded interface modeshapes 13 to 24. In this sense, negligible modal property is missed while using tuned loaded interface modeshape.

Another comparison is made between the eigenvectors corresponding to the nonlinear DOFs, obtained from the final ROM. In one of which, mistuned loaded interface modeshapes are used as one of the reduction basis. The diagonal MAC of the final ROM eigenvectors corresponding to the retained nonlinear DOFs is shown in Fig. 10. Note that, modeshapes of ROMs corresponding to Fig. 8 are used in computation of the diagonal MAC. As can be seen, modeshape are in an excellent correlation (higher than 0.99) with each other. Thus, the ROMs obtained based on either mistuned or tuned loaded interface modeshapes, give practically identical eigenvectors.

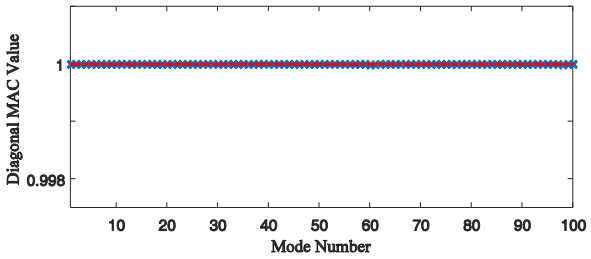

Fig. 10 Modal correlation between ROM eigenvectors based on tuned and mistuned loaded interface (LI) modes

3.5 Results based on tuned $\widehat{K}$ partition

As discussed in the mistuning modeling section, one assumption to simplify the mistuning introduction into the final reduced stiffness matrix is to neglect the effect of mistuning on the constraint modes corresponding to interface DOFs (i.e. considering a tuned $\widehat{K}$ partition in the K_{ROM}). The validity of this assumption is investigated here.

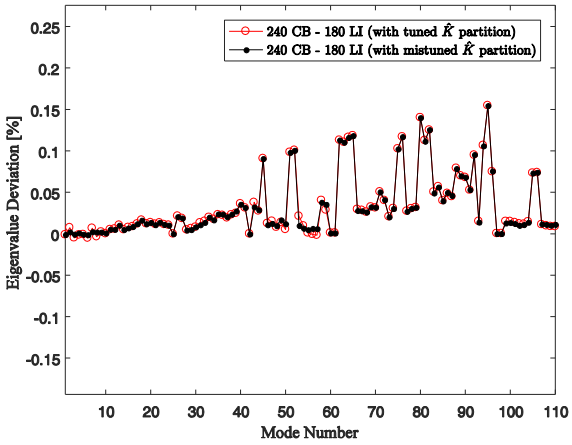

Fig. 11 The influence of neglecting the mistuning in $\widehat{K}$ partition on the accuracy of predicted eigenvalues by the ROM

Figure 11 shows the difference between exact natural frequencies of a mistuned bladed disk (obtained from full FE in ANSYS) and those obtained from two different ROMs. The red curve shows the results obtained from the ROM with a tuned $\widehat{K}$ partition while the black curve represents the ROM results with a mistuned $\widehat{K}$ partition. As it is seen, results of the ROM with tuned $\widehat{K}$ are in good accordance

with results of the ROM with mistuned $\widehat{K}$. In fact, due to the minimal contribution of interface DOFs to system dynamics, neglecting the effect of mistuning on them is a valid assumption.

3.6 Localized modeshapes

The presence of mistuning can result in localization of vibration modes. This confines the vibration energy around few number of blades and increases their vibration amplitude, significantly. The capability of the proposed reduction technique in accurately predicting the mode localization is assessed here. To this end, a localized vibration mode, namely 107th mistuned mode with corresponding natural frequency of 372 Hz, is studied. It is worth mentioning that the ROM predicted the mistuned eigenvalue by 0.0096% error. Figure 12 shows a comparison between localized modeshapes obtained by ROM and FE model, for the 107th mistuned modeshape. Only axial component of modal displacements of an identical contact node on each blade, is used to plot the modeshapes. As can be seen, the proposed ROM can accurately model the localized modeshape and its results coincide with exact FE result.

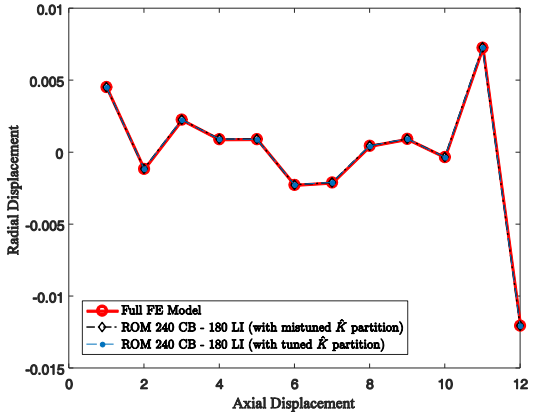

Fig. 12 Localized modeshapes obtained from ROM and FE model

3.7 Results for forced response analysis

For the nonlinear forced case, it is assumed that the global tangential and normal contact stiffnesses (i.e. k_{tx}, k_{ty} and k_n, respectively) have same values, and, the global tangential stiffness is uniformly

distributed among all local contact nodes. Here, the considered nominal values of the global contact stiffnesses are k_{tx}=k_{ty}=k_n=1e4 N/µm. The effect of static loads, are modeled by applying a constant normal preload (i.e. N0) on each contact node pair. Also, periodic external forces are modeled by a travelling wave type excitation of amplitude F0. Note that, two extra master nodes on each blade (located at the blade-shroud tip) are retained as the response and forcing nodes. The amplitude of the periodic response is computed based on a mono-harmonic balance procedure (only including the first harmonic). The tangential component of the periodic solution (calculated at the response node located on blade #1) is used to plot the forced response levels. In all forced cases, a viscous damping with damping ratio $\xi = 0.001$ (similar for all modes) is considered. A ROM comprised of 240 CB and 180 loaded interface modes, is used to carry out forced response computations.

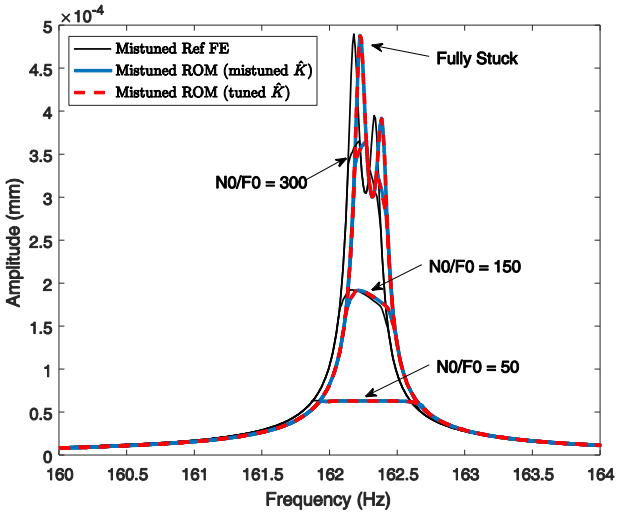

Fig. 13 Comparison of nonlinear forced response levels of mistuned ROMs and FE model (EO = 5)

The accuracy of the ROMs (one with tuned $\hat{K}$ and the other with mistuned $\hat{K}$) in predicting the nonlinear forced response levels of a mistuned turbine bladed disk under EO excitation 5 is depicted in Fig. 13. As the reference, a CB-CMS reduced FE model; by retaining a large number of CB modes (namely 1200 modes) and retaining the same master DOFs as in the ROMs; is considered. This system is referred to as the Ref FE and in the case of nonlinear forced response analyses, all ROM results are compared with the results of the so-called Ref FE. As it is seen in Fig. 13, forced response results of

the ROM with tuned $\widehat{K}$ is in an excellent accordance with the results of the ROM with mistuned $\widehat{K}$ partition. This indicates that the effect of blade frequency mistuning on interface DOFs are negligible. Moreover, the results of both ROMs are in a very good agreement with Ref FE results. The predicted peaks around the resonance are in excellent match with the Ref FE for different values of preload-to-excitation ratio (i.e. N0/F0). A very slight frequency shift (about 0.04 Hz or 0.025% error) is observed in the response levels predicted by ROMs, which is typical of reduced order models. It is evident from the figure, that decreasing the N0/F0 ratio will change the contact state from fully stick condition towards the gross slip. As a result, the increased damping introduced from the shrouds in microslip, decreases the response amplitudes.

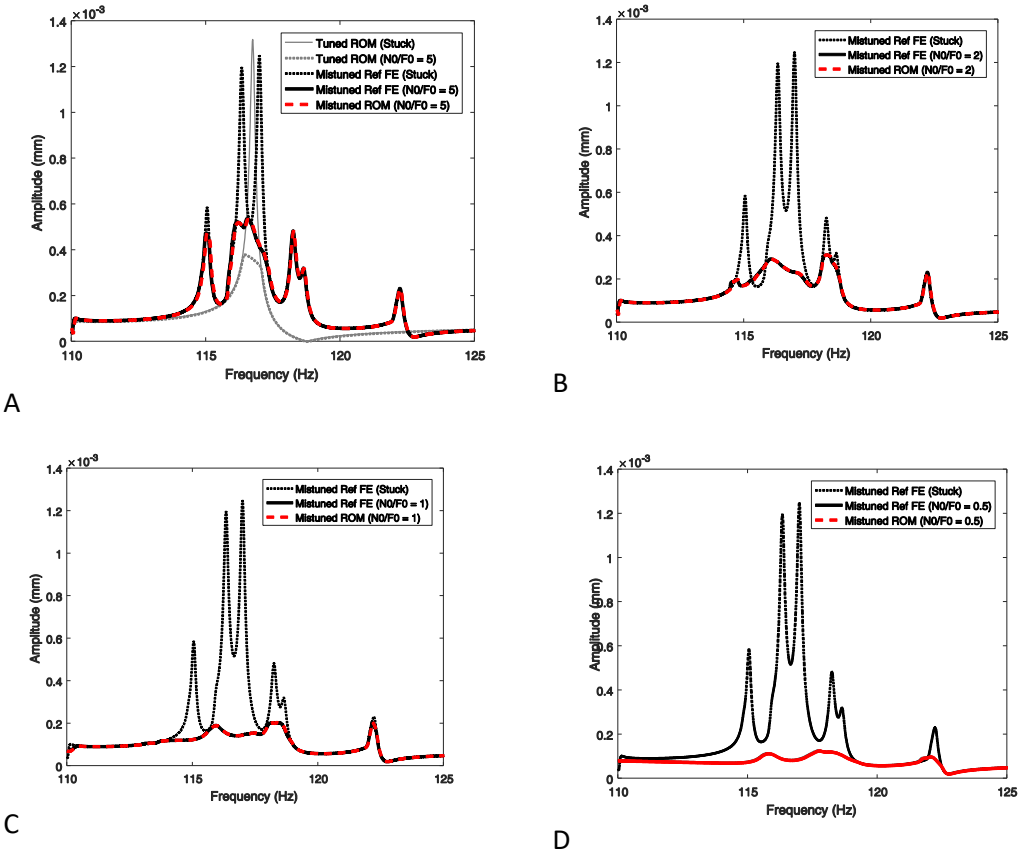

Fig. 14 Nonlinear forced response levels of the mistuned rom versus ref FE. a) N0/F0 = 5. b) N0/F0 = 2. c) N0/F0 = 1. d) N0/F0 = 0.5.

Nonlinear forced response levels for EO 5 excitation within a high modal density region are shown in Fig. 14. Results of the ROM with tuned $\widehat{K}$ is presented and compared with Ref FE results. It is expected that the ROM with mistuned $\widehat{K}$ partition will give results of the same/higher accuracy. The investigated

frequency range is selected near a softening region of Fig. 3 and it comprises multiple blade dominated modes. As discussed before (in Fig. 3), blades and shrouds within this frequency range experience complex dynamic motions, blades undergo a torsional motion which results in a wavy motion (with a dominant component along axial direction) in the coupled shrouds. In the mistuned system, other ND modeshapes besides ND 5, are also present in the selected range. The accuracy of the ROM in predicting the nonlinear forced response levels is evaluated in this frequency range. As it is seen, the forced response levels predicted by the ROM are in an excellent accordance with the Ref FE results. In Fig. 14(A), the response levels of the tuned bladed disk, both in fully stuck and microslip conditions, are shown. It is seen that the response level of the fully stuck tuned system is higher than that of the mistuned one (for this specific considered blade), and that, despite the engine order excitation, multiple peaks are present within the frequency range. Moreover, for the considered blade (namely blade #1) the mistuned nonlinear response level is higher than that of the tuned one. It is an interesting result, that in microslip conditions, the mistuning can increase the nonlinear damped response levels. It should be noted that, the investigated frequency range is far from blade-disk veering regions and in this frequency range, disk does not contribute to the system dynamics, significantly. The effect of preload-to-excitation ratio on the damping performance is evident in Figs. 14(A) to (D). For relatively higher values of N0/F0, it is seen that the contacts are in stick near low amplitude peaks and they behave like linear springs with no damping effects, while near high amplitude peaks, due to the higher relative displacements at contact nodes, the contacts are in microslip and the damping provided by the slip, decreases the periodic response amplitude. Further decreasing of N0/F0 values, increases the slip levels and as a result, the amplitude of the vibration is damped within the full frequency range.

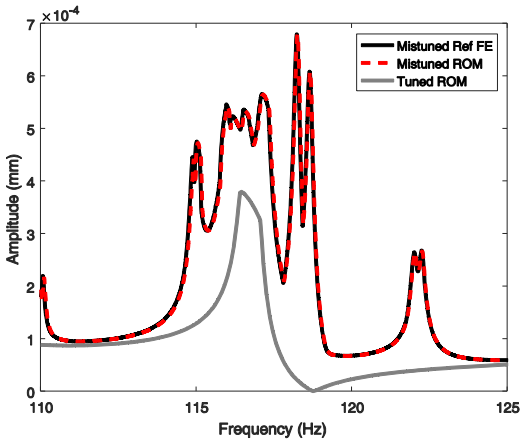

Fig. 15 Nonlinear response amplification of the mistuned bladed disk (EO =5 and N0/F0 =5)

Figure 15 demonstrates the response amplification phenomenon for a mistuned bladed disk in microslip condition. The system is under EO 5 excitation and N0/F0 is equal to 5. It is well known that, for linear systems, mistuning could increase the response levels. Here, the maximum nonlinear response of all blades is computed at each frequency. The depicted nonlinear response curve, is in fact the envelope of the maximum response of all blades. As it is seen the ROM (with tuned $\widehat{K}$) results are in excellent accordance with the Ref FE results. It is evident that, even in the presence of friction damping, the damped response of the mistuned system is increased by the amplification factor of 79% (with respect to the maximum response of the tuned system). It can be concluded that, since in the presence of friction damping, mistuning can increase the damped response levels by localizing the response around few number of blades, for an optimum design, the effect of mistuning and friction damping must be modeled simultaneously.

4 Conclusion

A new reduced order model for nonlinear dynamics of mistuned turbine bladed disks with shroud friction contacts was developed in this study. The novel reduction technique is based on small mistuning assumption (blade frequency mistuning). As a preliminary step, a single sector composed of one blade and the fundamental sector of the cyclic symmetry disk was considered. Based on the proposed reduction approach, a CB-CMS reduction was applied to the blade component, where

shroud contact DOFs and blade-disk interface DOFs were retained as master DOFs, and a modal reduction based on loaded interface modeshapes of the disk applied to the interface and disk components. Finally, it was shown how to extend the single sector results to the full structure. Based on the developed formulation, the reduced stiffness matrix of the mistuned system is computed by sector level calculations. Both linear analyses and nonlinear forced response results revealed the accuracy of the new reduction technique in predicting the dynamics of the mistuned system especially in high modal density regions. It was revealed that the mistuning can increase the damped response levels. It was shown that the effect of blade frequency mistuning on interface DOFs can be neglected without losing accuracy. This assumption, inevitably, results in a cheaper computational cost for statistical analyses. However, if deemed necessary by the analyst to take into account the effect of mistuning on interface DOFs, an exact formulation, based on sector level calculations, is provided with minimal computational cost, suitable for statistical analyses. In this research, the method was successfully applied to a mock-up bladed disk with shrouded blades, although the entire process can be applied to bladed disks with underplatform dampers. In that context, master DOFs during the CB-CMS blade reduction should comprise both the blade-disk and the blade-damper interface DOFs.

References

[1] Srinivasan, A. V. "Flutter and resonant vibration characteristics of engine blades." *Journal of engineering for gas turbines and power* 119, no. 4 (1997): 742-775.

[2] Seinturier, E. "Forced response computation for bladed disks industrial practices and advanced methods." *LECTURE SERIES-VON KARMAN INSTITUTE FOR FLUID DYNAMICS*2 (2007): 5.

[3] Ewins, D. J. "Control of vibration and resonance in aero engines and rotating machinery–An overview." *International Journal of Pressure Vessels and Piping* 87, no. 9 (2010): 504-510.

[4] Cardona, Alberto, Thierry Coune, Albert Lerusse, and Michel Geradin. "A multiharmonic method for non-linear vibration analysis." *International Journal for Numerical Methods in Engineering* 37, no. 9 (1994): 1593-1608.

[5] Krack, Malte, Loic Salles, and Fabrice Thouverez. "Vibration prediction of bladed disks coupled by friction joints." *Archives of Computational Methods in Engineering* 24, no. 3 (2017): 589-636.

[6] Castanier, Matthew P., and Christophe Pierre. "Modeling and analysis of mistuned bladed disk vibration: current status and emerging directions." *Journal of Propulsion and Power* 22, no. 2 (2006): 384-396.

[7] D'Souza, Kiran X., and Bogdan I. Epureanu. "A statistical characterization of the effects of mistuning in multistage bladed disks." *Journal of Engineering for Gas Turbines and Power* 134, no. 1 (2012): 012503.

[8] Yang, M-T., and J. H. Griffin. "A reduced order model of mistuning using a subset of nominal system modes." In *ASME 1999 International Gas Turbine and Aeroengine Congress and Exhibition*, pp. V004T03A032-V004T03A032. American Society of Mechanical Engineers, 1999.

[9] Lim, Sang-Ho, Ronnie Bladh, Matthew P. Castanier, and Christophe Pierre. "Compact, generalized component mode mistuning representation for modeling bladed disk vibration." *AIAA journal* 45, no. 9 (2007): 2285-2298.
[10] Vargiu, P., C. M. Firrone, S. Zucca, and M. M. Gola. "A reduced order model based on sector mistuning for the dynamic analysis of mistuned bladed disks." *International Journal of Mechanical Sciences* 53, no. 8 (2011): 639-646.
[11] Petrov, E. P., K. Y. Sanliturk, and D. J. Ewins. "A new method for dynamic analysis of mistuned bladed disks based on the exact relationship between tuned and mistuned systems." *Journal of Engineering for Gas Turbines and Power* 124, no. 3 (2002): 586-597.
[12] Feiner, Drew M., and J. H. Griffin. "A fundamental model of mistuning for a single family of modes." In *ASME Turbo Expo 2002: Power for Land, Sea, and Air*, pp. 953-964. American Society of Mechanical Engineers, 2002.
[13] Fitzner, Colin, Bogdan I. Epureanu, and Sergio Filippi. "Nodal energy weighted transformation: A mistuning projection and its application to FLADE™ turbines." *Mechanical Systems and Signal Processing* 42, no. 1-2 (2014): 167-180.
[14] Petrov, E. P., and D. J. Ewins. "Method for analysis of nonlinear multiharmonic vibrations of mistuned bladed discs with scatter of contact interface characteristics." In *ASME Turbo Expo 2004: Power for Land, Sea, and Air*, pp. 385-395. American Society of Mechanical Engineers, 2004.
[15] Duan, Yongliang, Chaoping Zang, and E. P. Petrov. "Forced response analysis of high-mode vibrations for mistuned bladed disks with effective reduced-order models." *Journal of Engineering for Gas Turbines and Power* 138, no. 11 (2016): 112502.
[16] Petrov, E. P. "Analysis of nonlinear vibrations upon wear-induced loss of friction dampers in tuned and mistuned bladed discs." In *ASME Turbo Expo 2013: Turbine Technical Conference and Exposition*, pp. V07AT32A005-V07AT32A005. American Society of Mechanical Engineers, 2013.
[17] Mitra, Mainak, Stefano Zucca, and Bogdan I. Epureanu. "Adaptive microslip projection for reduction of frictional and contact nonlinearities in shrouded blisks." *Journal of Computational and Nonlinear Dynamics* 11, no. 4 (2016): 041016.
[18] Mitra, Mainak, Stefano Zucca, and Bogdan I. Epureanu. "Effects of contact mistuning on shrouded blisk dynamics." In *ASME Turbo Expo 2016: Turbomachinery Technical Conference and Exposition*, pp. V07AT32A026-V07AT32A026. American Society of Mechanical Engineers, 2016.
[19] Castanier, Matthew P., Yung-Chang Tan, and Christophe Pierre. "Characteristic constraint modes for component mode synthesis." *AIAA journal* 39, no. 6 (2001): 1182-1187.
[20] Song, Sang Heon, Matthew P. Castanier, and Christophe Pierre. "Multi-stage modeling of turbine engine rotor vibration." In *ASME 2005 International Design Engineering Technical Conferences and Computers and Information in Engineering Conference*, pp. 1533-1543. American Society of Mechanical Engineers, 2005.
[21] Carassale, Luigi, and Mirko Maurici. "Interface Reduction in Craig–Bampton Component Mode Synthesis by Orthogonal Polynomial Series." *Journal of Engineering for Gas Turbines and Power* 140, no. 5 (2018): 052504.
[22] Hohl, Andreas, Christian Siewert, Lars Panning, and Jorg Wallaschek. "A substructure based reduced order model for mistuned bladed disks." In *ASME 2009 International Design Engineering Technical Conferences and Computers and Information in Engineering Conference*, pp. 899-906. American Society of Mechanical Engineers, 2009.
[23] Hohl, Andreas, Lars Panning, and Jorg Wallaschek. "Analysis of the Influence of Blade Pattern Characteristics on the Forced Response of Mistuned Blisks With a Cyclic CMS-Based Substructure Model." In *ASME 2010 10th Biennial Conference on Engineering Systems Design and Analysis*, pp. 443-455. American Society of Mechanical Engineers, 2010.
[24] Craig, Roy, and Mervyn Bampton. "Coupling of substructures for dynamic analyses." *AIAA journal* 6, no. 7 (1968): 1313-1319.
[25] Benfield, W. A., and R. F. Hruda. "Vibration analysis of structures by component mode substitution." *AIAA journal* 9, no. 7 (1971): 1255-1261.
[26] Cameron, T. M., and J. H. Griffin. "An alternating frequency/time domain method for calculating the steady-state response of nonlinear dynamic systems." *Journal of applied mechanics* 56, no. 1 (1989): 149-154.
[27] Siewert, Christian, Lars Panning, Jörg Wallaschek, and Christoph Richter. "Multiharmonic forced response analysis of a turbine blading coupled by nonlinear contact forces." *Journal of Engineering for Gas Turbines and Power* 132, no. 8 (2010): 082501.
[28] Olson, Brian J., Steven W. Shaw, Chengzhi Shi, Christophe Pierre, and Robert G. Parker. "Circulant matrices and their application to vibration analysis." *Applied Mechanics Reviews*66, no. 4 (2014): 040803.

Appendix A: Direct Sum of Matrices

The direct sum of two matrices of arbitrary size is defined as:

$$A \oplus B = \begin{bmatrix} A & 0 \\ 0 & B \end{bmatrix} = \begin{bmatrix} a_{11} & \cdots & a_{1n} & 0 & \cdots & 0 \\ \vdots & \ddots & \vdots & \vdots & \ddots & \vdots \\ a_{m1} & \cdots & a_{mn} & 0 & \cdots & 0 \\ 0 & \cdots & 0 & b_{11} & \cdots & b_{1q} \\ \vdots & \ddots & \vdots & \vdots & \ddots & \vdots \\ 0 & \cdots & 0 & b_{p1} & \cdots & b_{pq} \end{bmatrix} \quad \text{A1}$$

Appendix B: Reduced mass matrix construction

Mass matrices in each reduction step are partitioned exactly in the same way as their corresponding reduced stiffness matrices. A more detailed description for mass matrices are given here. Accordingly, different partitions of M_{CB} are:

$$M_{cb}^{b} = \begin{bmatrix} m_{cb,NN}^{b} & m_{cb,N\gamma}^{b} \\ m_{cb,\gamma N}^{b} & m_{cb,\gamma\gamma}^{b} \end{bmatrix} \quad \text{B1}$$

where:

$$\begin{aligned} & m_{cb,NN}^{b} = \\ & m_{NN}^{b} + \left(k_{NI}^{b} k_{II}^{b^{-1}}\right) m_{II} \left(k_{II}^{b^{-1}} k_{IN}^{b}\right) - m_{NI} \left(k_{II}^{b^{-1}} k_{IN}^{b}\right) - \left(k_{NI}^{b} k_{II}^{b^{-1}}\right) m_{IN} \\ & m_{cb,\gamma\gamma}^{b} = \\ & m_{\gamma\gamma}^{b} + \left(k_{\gamma I}^{b} k_{II}^{b^{-1}}\right) m_{II} \left(k_{II}^{b^{-1}} k_{I\gamma}^{b}\right) - m_{\gamma I} \left(k_{II}^{b^{-1}} k_{I\gamma}^{b}\right) - \left(k_{\gamma I}^{b} k_{II}^{b^{-1}}\right) m_{I\gamma} \\ & m_{cb,N\gamma}^{b} = \\ & \left(k_{NI}^{b} k_{II}^{b^{-1}}\right) m_{II} \left(k_{II}^{b^{-1}} k_{I\gamma}^{b}\right) - m_{NI} \left(k_{II}^{b^{-1}} k_{I\gamma}^{b}\right) - \left(k_{NI}^{b} k_{II}^{b^{-1}}\right) m_{I\gamma} \\ & m_{cb,\gamma N}^{b} = \\ & \left(k_{\gamma I}^{b} k_{II}^{b^{-1}}\right) m_{II} \left(k_{II}^{b^{-1}} k_{IN}^{b}\right) - m_{\gamma I} \left(k_{II}^{b^{-1}} k_{IN}^{b}\right) - \left(k_{\gamma I}^{b} k_{II}^{b^{-1}}\right) m_{IN}. \end{aligned} \quad \text{B2}$$

Implementing the same procedure as for stiffness matrix, final reduced mass matrix of a single sector yields:

$$M_{rom}=\begin{bmatrix} I & m_{\eta N} & 0 \\ m_{N\eta} & m^b_{cb,NN} & m^b_{cb,N\gamma}\tilde{\varphi}_\gamma \\ 0 & \tilde{\varphi}^T_\gamma m^b_{cb,\gamma N} & [\hat{m}] \end{bmatrix}$$

B3

where

$$\hat{m}=\begin{bmatrix}\tilde{\varphi}_\gamma \\ \tilde{\varphi}_O\end{bmatrix}^T\begin{bmatrix} m^b_{cb,\gamma\gamma}+m^d_{\gamma\gamma} & m^d_{\gamma O} \\ m^d_{O\gamma} & m^d_{OO}\end{bmatrix}\begin{bmatrix}\tilde{\varphi}_\gamma \\ \tilde{\varphi}_O\end{bmatrix}.$$

B4

One may obtain the final reduced stiffness matrix of the full system, as follows:

$$M_{ROM}=\begin{bmatrix} I\otimes\Lambda^b_i & I\otimes m_{N\eta} & 0 \\ I\otimes m_{N\eta} & I\otimes m^b_{cb,NN} & \left(I\otimes m^b_{cb,N\gamma}\right)\tilde{\Phi}_\gamma \\ 0 & \tilde{\Phi}^T_\gamma\left(I\otimes m^b_{cb,\gamma N}\right) & [\hat{M}] \end{bmatrix}$$

$$\hat{M}=\begin{bmatrix}\tilde{\Phi}_\gamma \\ \tilde{\Phi}_O\end{bmatrix}^T\begin{bmatrix} \underset{n=1..N}{Bdiag}[m^{rom^{(n)}}_{\gamma\gamma}] & I\otimes m^d_{\gamma O} \\ I\otimes m^d_{O\gamma} & \bar{m}^d_{OO}\end{bmatrix}\begin{bmatrix}\tilde{\Phi}_\gamma \\ \tilde{\Phi}_O\end{bmatrix}$$

B5

where $\underset{n=1..N}{Bdiag}[m^{rom^{(n)}}_{\gamma\gamma}]=I\otimes m^{rom}_{\gamma\gamma}=I\otimes\left(m^b_{cb,\gamma\gamma}+m^d_{\gamma\gamma}\right)$. Finally, the alternative formulation for $\hat{M}$ is expressed below. Using the operator introduced by Eqn. (29), the compact notation for $\hat{M}$ takes the following form:

$$\hat{M}=\tilde{\Phi}^T\left(M_D+blkdg[m^b_{cb,\gamma\gamma}]\right)\tilde{\Phi}$$

B6

By adding and subtracting the Guyan mass matrix of the tuned blades to the interface DOFs of the $\hat{M}$ central core and using Eqn. (B6), one may cast $\hat{M}$ as follows:

$$\begin{aligned}&\hat{M}\\ &=\tilde{\Phi}^T\left(M_D+blkdg[m^b_{Guyan}]-blkdg[m^b_{Guyan}]+blkdg[m^b_{cb,\gamma\gamma}]\right)\tilde{\Phi}\\ &=\tilde{\Phi}^T\left(\tilde{M}-blkdg[m^b_{Guyan}]+blkdg[m^b_{cb,\gamma\gamma}]\right)\tilde{\Phi}\\ &=[I]-\tilde{\Phi}^T_\gamma\underset{n=1..N}{Bdiag}[m^{b^{(n)}}_{Guyan}]\tilde{\Phi}_\gamma+\tilde{\Phi}^T_\gamma\underset{n=1..N}{Bdiag}[m^{b^{(n)}}_{cb,\gamma\gamma}]\tilde{\Phi}_\gamma\end{aligned}$$

B7

Note this alternative formulation enables constructing the final reduced mass matrix by sector level calculations.